MULTIBODY DYNAMICS 2011, ECCOMAS Thematic Conference
J.C. Samin, P. Fisette (eds.)
Brussels, Belgium, 4-7 July 2011

OPTIMIZATION OF FLEXIBLE COMPONENTS IN RECIPROCATING ENGINES WITH CYCLIC DYNAMIC LOADING

Emmanuel Tromme, Olivier Brüls and Pierre Duysinx

Department of Aerospace and Mechanical Engineering (LTAS)
University of Liège, Chemin des chevreuils 1, Building B52, 4000 Liège
e-mails: emmanuel.tromme@ulg.ac.be, o.bruls@ulg.ac.be, p.duysinx@ulg.ac.be,
web page: http://www.ltas.ulg.ac.be

Keywords: Shape optimization, cyclic dynamic loading, flexible multibody system.

Abstract. *This work considers the optimization of flexible components of mechanical systems modeled as multibody systems. This approach permits to better capture the effects of dynamic loading under service conditions. This process is challenging because most state-of-the-art studies in structural optimization have been conducted under static or quasi-static conditions. The formulation of the optimization problem for dynamic systems is fundamental; it is not a simple extension of static optimization. Naive implementation leads to fragile and unstable results. The present paper addresses the optimization of a connecting rod of a reciprocating engine with cyclic dynamic loading. Gradient-based methods are adopted for their convergence speed. Different formulations are investigated and compared. A first numerical application considers the optimization of the connecting rod regarding its mass and its elongation. After, another numerical application is carried on considering the stresses in the connecting rod. A conclusion on the influence of the optimization problem formulation is realized.*

1 INTRODUCTION

Since the early sixties, many works and efforts have been realized in the field of structural optimization. Nowadays, sizing and shape optimizations are commonly used for industrial applications while topology optimization is more employed in the industry as a tool in a pre-design phase. Topology optimization is not only dedicated to increase the rigidity of a structure while minimizing its mass but it has applications in a multitude of fields: design of compliant mechanisms, electromagnetism, fluid flow, wave propagation,... and architecture (See for instance the Qatar National Convention Center). In topology optimization problems, it has been noticed that the optimal design may be very sensitive to the supports and loading conditions [1].

While in the real world the majority of loads are dynamic, structural optimization has been applied to the design of components under (quasi-)static or vibration design criteria. This simplification is originated from the difficulties of dealing with dynamic response optimization.

Mechanical systems consist generally of components, interconnected by joints and force elements, which undergo large displacements, translations and rotations. For instance, typical systems are space structures, vehicles and robots. Those systems can be modeled as flexible multibody systems and analyzed using commercial simulation tools.

In Ref. [2], at the beginning of the optimization of mechanical systems, the considered component for the optimization is isolated from the system, then multiple static postures are selected for the optimization process. This approach is doubtful because a few postures cannot represent the overall system motion of a high-speed system. Moreover, the coupling between rigid and elastic motions are omitted which causes an inaccuracy on the displacements and on the stresses. Another point is that the multiple static postures do not account for the time-dependency of the constraints. Finally, the static postures were chosen in a non-rational way.

Nowadays, a classical approach to carry out the component dynamic optimization is to reformulate the dynamic multibody system problem as a set of static problems. Indeed, the optimization techniques of static problems are well established. This procedure consists of two steps: first a rigid MBS simulation precomputes the loads applied to each component, afterwards each component is optimized independently using a quasi-static approach. A set of equivalent static load cases should therefore be defined in order to mimic the precomputed dynamic loads. Oral and Ider [3] were among the first to use this technique to optimize a high speed robotic arms and they used the most critical constraints for the equivalent constraints. Haussler *et al.* [4] derived some load cases from the rigid MBS simulation in order to use them in the structural optimization of each component. They applied this method to optimize the spindle carrier of a turning machine and they compared this approach to a conventional static method where the spindle carrier motion was neglected and the load updates were not taken into account. In the case of the topology optimization of accelerated components within a mechanical system, Haussler *et al.* [5], using this two steps method, showed that it is important to consider the changes of the boundary conditions and system behavior during optimization since these are subject to significant changes. Kang and Park [6] used the component mode approach to define more precisely quasi-static load cases in the case of sizing optimization. A last example, Hong *et al.* [7] proposed a method to design large-scale flexible multibody systems with a reasonable computation time and acceptable accuracy of the results. They employed rigid multibody dynamic analysis (to reduce computation time) and the equivalent static loads.

Concerning this equivalent static loads approach, one can point out that the method ignores the component interactions, the global vibration behavior of the mechanism and that the modeling of high frequency loadings is poor.

In modern mechanical engineering, MBS simulations are widely employed to analyze the behavior of the complete mechanical system. However, most of the MBS dynamic formalisms are based on rigid body assumptions and they are not completely suitable to be extended to take into account the full flexibility of the components. Recently, a strong tendency to merge both finite element (FE) analysis and MBS simulation into an unified code has been followed. Software tools resulting from this tendency allow analyzing the deformations of mechanism undergoing fast joint motions. An example of this type of software is SAMCEF Mecano which is able to account for MBS joints in non-linear FE models and which results from the work of Géradin and Cardona [8].

Brüls *et al.* [9] took advantages of the evolution of numerical simulations and topology optimization codes in order to design optimal structural components loaded during the MBS motion. They validated this method and showed that it is more convenient to work with an optimization loop directly based on the dynamic response of the flexible multibody system to obtain a more integrated approach. Running on from this work, Duysinx *et al.* [10] investigated the "fully integrated" optimization problem of flexible components under dynamic loading conditions. The approach was illustrated on numerical applications of mass optimization of robotic arms subjected to constraints on the trajectory tracking.

The optimization of MBS is not a simple extension of structural optimization [9, 10]. The coupled problem between vibrations and interaction within the components generally results in complex design problems and convergence difficulties. The design problem is complicated, and naive implementations lead to fragile and unstable results. To overcome this problem, it is crucial to formulate the problem in a correct way. The way that the time-dependent constraints are taken into account is fundamental for the convergence of the problem. Furthermore, whether a feasible starting point is available or not, gradient-based solvers can converge efficiently or not.

This work continues with the same idea, *i.e.* the MBS modeling tackles the dynamic effects while the FE discretization of the components accounts naturally for the flexibility in MBS components and possibly joints. An integrated structural optimization technique is developed for reciprocating engines with cyclic dynamic loading.

The connecting rod is an essential element in a reciprocating engine. It is the component which transforms the translational movement of the piston into a rotational movement for the wheels. This element is subject to a lot of stresses during its life. An important point is that the connecting rod must be sufficiently stiff to transmit the motion after the gas explosion but also not to elongate too much during the exhaust phase to prevent the collision with the valves. The number of cycles that a connecting rod undergoes during its life is very large and it is critical to take into account the fatigue strength as well as its critical buckling load during its design.

Flexible MBS simulations allow estimating precisely the dynamic loading. However, considering the stress constraints in each finite element at every integration time step makes the optimization problem very large. In this study, thanks to the cyclic behavior of the reciprocating engine and to the identification of a critical instant, it is possible to take into account the stress constraints in the optimization process while the computation time is still small.

This study is dedicated to shape optimization of a connecting rod which is parametrized. This is a step further in the "fully integrated" approach since previous applications considered academic examples to validate and to investigate the method [9, 10]. This study extends the "fully integrated" approach to a more realistic case.

The first part of the paper is dedicated to recall the flexible MBS modeling, the time integration method, optimization algorithm and sensitivity analysis. After, a discussion on the

formulation of the optimization problem is performed. Finally, numerical applications on the optimization of a connecting rod in a reciprocating engine with cyclic dynamic loading are developed. Conclusions and perspectives close the discussion.

2 FLEXIBLE MULTIBODY SYSTEMS SIMULATION

2.1 Equations of motion of flexible multibody dynamic systems

In previous works, the flexibility of the multibody system was accounted by Component Mode Synthesis approach [6] or was simply neglected for the MBS simulation to reduce computation time for large-scale model and reintroduced later [7].

In this work, flexible multibody systems are modeled using a non-linear finite element formulation, as suggested by Géradin and Cardona [8].

The formulation is based on an inertial frame approach. Absolute nodal coordinates which are gathered in the vector $\mathbf{q}$ are employed to represent the motion of each flexible body. In other words, the vector $\mathbf{q}$ contains the displacement and orientation of each node of the finite element mesh.

The motion of the mechanical system is not completely free and is subject to kinematic constraints, noted $\mathbf{\Phi}(\mathbf{q}) = \mathbf{0}$, which typically ensure the connection between the different bodies at joints. They impose non-linear kinematic constraints between nodal coordinates. Different possibilities exist to solve this type of problem and in SAMCEF Mecano, the constrained dynamic problem is formulated using an augmented Lagrangian approach.

Let assume that we know the potential energy of external forces $\mathcal{V}(\mathbf{q})$, the deformation energy of elastic bodies $\mathcal{W}(\mathbf{q})$ and the kinetic energy defined by

$$\mathcal{K}(\mathbf{q}, \dot{\mathbf{q}}) = \frac{1}{2}\dot{\mathbf{q}}^T \mathbf{M}(\mathbf{q})\, \dot{\mathbf{q}} \tag{1}$$

where the $n \times n$ symmetric mass matrix $\mathbf{M}$ may depend on the generalized coordinates. The Lagrangian function of the conservative system is defined by

$$\mathcal{L}(\mathbf{q}, \dot{\mathbf{q}}) = \mathcal{K}(\mathbf{q}, \dot{\mathbf{q}}) - \mathcal{V}(\mathbf{q}) - \mathcal{W}(\mathbf{q})\,. \tag{2}$$

The motion equations of the system are derived by combining the Hamilton principle with the Lagrangian function Eq. (2). After some calculations (see for instance Ref. [11]), the Lagrange equations of motion for a dynamic system subjected to holonomic constraints are stated as follows

$$\frac{d}{dt}\left(\frac{\partial \mathcal{L}}{\partial \dot{\mathbf{q}}}\right) - \frac{\partial \mathcal{L}}{\partial \mathbf{q}} = \boldsymbol{\mathcal{Q}}, \qquad \mathbf{\Phi}(\mathbf{q}) = \mathbf{0}. \tag{3}$$

where $\boldsymbol{\mathcal{Q}}$ represents the internal forces of constraints. With the classical Lagrangian approach, the constraint forces take the following form

$$\boldsymbol{\mathcal{Q}}_i = \boldsymbol{\lambda}^T \frac{\partial \mathbf{\Phi}}{\partial \mathbf{q}_i}. \tag{4}$$

When employing an augmented Lagrangian approach, a penalty term is added in the formulation of the constraint forces in particular for convergence reasons (Ref. [12]). With this approach, the constraint forces become

$$\boldsymbol{\mathcal{Q}}_i = \left(k\boldsymbol{\lambda} - p\mathbf{\Phi}\right)^T \frac{\partial \mathbf{\Phi}}{\partial \mathbf{q}_i} \tag{5}$$

where k and p are a scale and a penalty factors, respectively.

Finally, after developments, the equations of motion take the general form of a differential algebraic system (DAE)

$$\mathbf{M}(\mathbf{q})\,\ddot{\mathbf{q}} + \mathbf{g}^{gyr}(\mathbf{q},\dot{\mathbf{q}}) + \mathbf{g}^{int}(\mathbf{q}) + \mathbf{\Phi}_{\mathbf{q}}^{T}(\mathbf{q},t)\,(k\boldsymbol{\lambda} + p\mathbf{\Phi}) = \mathbf{g}^{ext}(\mathbf{q}) \quad (6)$$

$$k\mathbf{\Phi}(\mathbf{q}) = \mathbf{0} \quad (7)$$

The subscript $_{\mathbf{q}}$ denotes the derivative with respect to $\mathbf{q}$. Equation (6) represents the dynamic equilibrium while equation (7) corresponds to the kinematic constraints. As noticed before, the mass matrix $\mathbf{M}$ may depend on the generalized coordinates and is not constant in case of large rotations. $\mathbf{g}^{int}$, $\mathbf{g}^{ext}$ and $\mathbf{g}^{gyr}$ stand for the internal forces, the external forces and the gyroscopic-centrifugal forces respectively.

2.2 Time integration

Géradin and Cardona suggested that the set of non-linear differential algebraic equations can be solved using the generalized-α method developed by Chung and Hulbert [13]. Arnold and Brüls [14] have demonstrated that, despite the presence of algebraic constraints and despite the non-constant character of the mass matrix, this integration scheme leads to accurate and reliable results with a small amount of numerical damping. At time step $n+1$, the numerical variables $\ddot{\mathbf{q}}_{n+1}$, $\dot{\mathbf{q}}_{n+1}$, $\mathbf{q}_{n+1}$ and $\boldsymbol{\lambda}_{n+1}$ have to satisfy the system of equations (6-7). According to the generalized-α method, a vector $\mathbf{a}$ of acceleration-like variables is defined by the following recurrence relation

$$(1-\alpha_m)\,\mathbf{a}_{n+1} + \alpha_m \mathbf{a}_n = (1-\alpha_f)\,\ddot{\mathbf{q}}_{n+1} + \alpha_f \ddot{\mathbf{q}}_n, \qquad \mathbf{a}_0 = \ddot{\mathbf{q}}_0 \quad (8)$$

The integration scheme is obtained by employing $\mathbf{a}$ in the Newmark integration formulae:

$$\mathbf{q}_{n+1} = \mathbf{q}_n + h\dot{\mathbf{q}}_n + h^2\left(\frac{1}{2}-\beta\right)\mathbf{a}_n + h^2\beta\mathbf{a}_{n+1} \quad (9)$$

$$\dot{\mathbf{q}}_{n+1} = \dot{\mathbf{q}}_n + h\,(1-\gamma)\,\mathbf{a}_n + h\gamma\mathbf{a}_{n+1} \quad (10)$$

where h denotes the time step. If the parameters α_f, α_m, β and γ are properly chosen according to Chung ad Hulbert [13], second-order accuracy and linear unconditional stability are guaranteed. Going one time step further requires to solve iteratively the dynamic equilibrium at time t_{n+1}. This is performed by using the linearized form (Eqs. (11-12)) of equations (6-7) and by employing the Newton-Raphson method. The iterations try to bring the residual $\mathbf{r} = \mathbf{M}\ddot{\mathbf{q}} - \mathbf{q} + \mathbf{\Phi}_{\mathbf{q}}^{T}\boldsymbol{\lambda}$ and $\mathbf{\Phi}$ to zero.

$$\mathbf{M}\Delta\ddot{\mathbf{q}} + \mathbf{C}_t\Delta\dot{\mathbf{q}} + \mathbf{K}_t\Delta\mathbf{q} + \mathbf{\Phi}_{\mathbf{q}}^{T}\Delta\boldsymbol{\lambda} = \Delta\mathbf{r} \quad (11)$$

$$\mathbf{\Phi}_{\mathbf{q}}\Delta\mathbf{q} = \Delta\mathbf{\Phi} \quad (12)$$

where $\mathbf{C}_t = \partial\mathbf{r}/\partial\dot{\mathbf{q}}$ and $\mathbf{K}_t = \partial\mathbf{r}/\partial\mathbf{q}$ denote the tangent damping and stiffness matrices respectively.

3 OPTIMIZATION OF FLEXIBLE MULTIBODY SYSTEMS

3.1 General statement of the optimization problem

The general statement of an optimization problem (Eq. (13)) consists in minimizing an objective function $f(\mathbf{x})$ subjected to some constraints $g_j(\mathbf{x})$ which typically insure the feasibility

of the structural design. The vector $\mathbf{x}$ contains the design variables which are the parameters that are modified during the optimization process. Side-constraints limit the values taken by the design parameters and reflect technological considerations.

$$\begin{min_{\mathbf{x}} f(\mathbf{x}) \\ s.t. \begin{cases} g_j(\mathbf{x}) \leq \overline{g}_j, & j = 1, \ldots, m \\ \underline{x}_i \leq x_i \leq \overline{x}_i, & i = 1, \ldots, n \end{cases}} \tag{13}$$

This formulation allows using many different optimization algorithms to solve the problem. It is completely general and there is no need to develop specific method. Moreover, this formulation provide a general and robust framework to the solution procedure.

In our case, the function $f(\mathbf{x})$ and $g_j(\mathbf{x})$ are structural responses like mass, displacements and stresses for instance. The design parameters x_i are shape parameters.

3.2 Optimization algorithm

Going back to 1847 with the initial work of Cauchy, one can say that the gradient method is probably one of the oldest optimization algorithms. With the power improvement of computer technology and the desire to solve larger and larger scale problems, the gradient method had renewed interest during the second part of the twentieth century.

In this study, only mathematical programming (MP) methods which require to compute the derivative of the design function are considered. These methods have been employed to solve large scale structural and multidisciplinary optimization problems with conclusive results. The convergence speed is very high and allows obtaining an optimal solution within a limited number of iterations and function evaluations. The inconvenient of these methods is that they provide local optima due to the local convergence properties. Another inconvenient is that following the non-linear behavior of the problem, the robustness of MP algorithms can be a source of difficulties.

The algorithm adopted for this study is GCMMA [15]. It is an extension of CONLIN [16] and MMA [17] algorithms based on the sequential convex programming approach. It consists of adjusting the degree of convexity to suit the particular problem. In CONLIN algorithm, direct and reciprocal variables are used while in GCMMA, intermediate variables are employed which involves the specification of moving asymptotes. One of the extensions from MMA algorithm is that both asymptotes can be activated simultaneously in order to create non-monotonous approximations.

Generally, the optimization problems are non-linear and implicit with respect to the design variables. As the number of function evaluations to solve the problem can be quite important, it is convenient to build approximations of the actual functions and to use an iterative process to solve the actual optimization problem.

In fact, the actual optimization problem is replaced by a sequence of explicit and convex subproblems which are built on local approximations of the design functions. Then, each explicit and convex subproblem is solved using fast and efficient mathematical programming algorithms such as for instance the Lagrangian maximization (dual method). This way permits to reduce drastically the computation time.

In the case of GCMMA, the explicit approximation of a function g_j is:

$$g_j(\mathbf{x}) \approx c_j + \sum_{+} \frac{p_{ij}}{u_{ij} - x_i} + \sum_{-} \frac{q_{ij}}{x_i - l_{ij}} \tag{14}$$

The index of the summation sign indicates that, according to the sign of $\partial g_j\left(\mathbf{x}^k\right)/\partial x_i$, the coefficient p_{ij} or q_{ij} is used. The values of p_{ij} and q_{ij} are always strictly positive. The lower and upper asymptotes are respectively l_{ij} and u_{ij}. To define the coefficients, an internal parameter ρ_j is introduced for each function:

$$p_{ij} \approx \left(\frac{\partial g_j\left(\mathbf{x}^k\right)}{\partial x_i} + \left(\frac{\rho_j}{2}\right)(u_{ij} - l_{ij})\right)\left(u_{ij} - x_i^k\right)^2, \qquad \text{with} \frac{\partial g_j\left(\mathbf{x}^k\right)}{\partial x_i} > 0 \tag{15}$$

$$q_{ij} \approx \left(\frac{\partial g_j\left(\mathbf{x}^k\right)}{\partial x_i} + \left(\frac{\rho_j}{2}\right)(u_{ij} - l_{ij})\right)\left(x_i^k - l_{ij}\right)^2, \qquad \text{with} \frac{\partial g_j\left(\mathbf{x}^k\right)}{\partial x_i} < 0 \tag{16}$$

$$c_j \approx g_j\left(\mathbf{x}^k\right) - \sum_{+} \frac{\partial g_j\left(\mathbf{x}^k\right)}{\partial x_i}\left(u_{ij} - x_i^k\right) + \sum_{-} \frac{\partial g_j\left(\mathbf{x}^k\right)}{\partial x_i}\left(x_i^k - l_{ij}\right) \tag{17}$$

The exponent k denotes the k^{th} iteration. The convergence of the method has been proved with a correct choice of the internal parameters. Moreover, this method is able to solve problems involving non-monotonous functions.

3.3 Sensitivity analysis

As a gradient-based optimization method is employed, a sensitivity analysis is necessary to compute the first order derivatives of the structural responses and to provide them to the optimization algorithm so that it can determine the descent direction. This part of the optimization process is crucial especially when the number of variables becomes important. Indeed, the computation time can increase strongly as the sensitivities have to be evaluated at each converged time step.

A first idea to compute the sensitivities is to employ a finite differences scheme. However, in this case, the sensitivity analysis requires one (or two for central difference) additional simulation per perturbed design variable. Despite its computational inefficiency, when the number of variables and the simulation time are small, this method can be used to carry out, for instance, a feasibility study.

When the simulation time increases and/or the number of design variable becomes larger, this method is unadapted and it is better to develop an analytical or semi-analytical sensitivity analysis. A semi-analytical approach based on a direct differentiation method is presented below. In other words, the sensitivities are computed by differentiation of the time integration algorithm.

For a given design variable x_j, the notation f' represents $\partial f/\partial x_j$. By using a chain rule of differentiation, the set of state equations (6) and kinematic constraints (7) are derived :

$$\mathbf{M}\ddot{\mathbf{q}}' + \mathbf{C}_t\dot{\mathbf{q}}' + \mathbf{K}_t\mathbf{q}' + \mathbf{\Phi}_\mathbf{q}^T\boldsymbol{\lambda}' + \mathbf{r}_{,x_j} = \mathbf{0} \tag{18}$$

$$\mathbf{\Phi}_\mathbf{q}\mathbf{q}' + \mathbf{\Phi}_{,x_j} = \mathbf{0} \tag{19}$$

where $\mathbf{r}_{,x_j}$ and $\mathbf{\Phi}_{,x_j}$, sometimes referred to as pseudo-loads, represent the partial derivatives of $\mathbf{r}$ and $\mathbf{\Phi}$ with respect to the parameter x_j.

By observing equations (18-19), one remarks that they are linear with respect to $\ddot{\mathbf{q}}'$, $\dot{\mathbf{q}}'$, $\mathbf{q}'$ and $\boldsymbol{\lambda}'$ while the dynamic equilibrium is non-linear with respect to $\ddot{\mathbf{q}}$, $\dot{\mathbf{q}}$, $\mathbf{q}$ and $\boldsymbol{\lambda}$. To compute the sensitivities at time $n+1$, the same integration algorithm as for the dynamic response can be used except that the residual $\mathbf{r}$ and $\mathbf{\Phi}$ are replaced by $\mathbf{r}_{,x_j}$ and $\mathbf{\Phi}_{,x_j}$. Since equations (18-19) are linear, a single Newton iteration is sufficient to get the exact values of the sensitivities.

In particular, the iteration matrix is the same as in the original problem. Therefore, it does not matter if a large number of design parameters are present because this matrix has to be computed and factorized only once for the sensitivity analysis at time $n+1$. A last remark is that though an approximate iteration matrix is often sufficient to obtain convergence for the original problem, it is necessary to have an exact expression to solve the sensitivity problem in one iteration. In this paper, the finite difference scheme is used.

The reference [18] gives a complete and detailed explanation of this sensitivity analysis.

4 OPTIMIZATION PROBLEM FORMULATION

The formulation of an optimization problem for multibody systems with rigid and flexible components is not trivial. Indeed, due to inertia effects, vibrations, design variables depending-loading, etc, the problem becomes extremely complex. As pointed out in previous works [9, 10], the problem must be carefully formulated to obtain a stable convergence and a robust optimization scheme. The objective function and the constraints have to be formulated in a way that it reflects the engineering approach of the design at best.

When optimizing a mechanism, different types of design variables can be adopted to perform the optimization process. In this study, the position of connections and joints, the length of links as well as the topology is kept unchanged. The design variables considered are some shape parameters of the components.

Generally, to ensure a certain precision of the motion, a formulation based on the maximization of the stiffness or the minimization of the compliance under the dynamic loading is employed. By similarity of the topology optimization, one can minimize the compliance of component i at time t

$$C_{(i)}\left(\mathbf{x},t\right)=\int_{V_E}\boldsymbol{\varepsilon}^T\left(\mathbf{x},t\right)\mathbf{D}\,\boldsymbol{\varepsilon}\left(\mathbf{x},t\right)\,dV \tag{20}$$

where $\boldsymbol{\varepsilon}$ denotes the strain tensor, $\mathbf{D}$ is the Hooke tensor and $\mathbf{x}$ represents the design variables vector. Brüls *et al.* [9] used this approach and suggested that for mechanical systems, one should consider the averaged compliance of all bodies estimated over a sufficiently long integration time T.

$$\overline{C}\left(\mathbf{x}\right)=\frac{1}{T}\int_0^T\sum_i C_{(i)}\left(\mathbf{x},\tau\right)d\tau \tag{21}$$

The advantage of this compliance formulation is that this measure is positive and therefore, by minimizing the compliance, the deflections of the mechanism are minimized. However, when the damping is small, the number of oscillations to come to a stationary behavior can be very large so that the reference time T must be taken very long.

Depending on the mechanism and on design considerations, different formulations more specific to the treated problem can be considered. When an ideal behavior is known, the formulation can compare the actual behavior to the ideal one. In this case, a function Δl is introduced to measure the difference between the two behaviors. This function can be considered as the objective function or can be treated as a constraint

$$\Delta l\left(\mathbf{x},t\right)\leq\Delta l_{max},\qquad\forall\, t\in\left[0,T\right]. \tag{22}$$

After time discretization, the expression becomes

$$\Delta l\left(\mathbf{x},t_i\right)\leq\Delta l_{max},\qquad\forall\, i=1,\ldots,n. \tag{23}$$

Generally, the mass is introduced in the formulation of an optimization problem. The mass is defined as

$$m = \int_{V_E} \rho \, dV \tag{24}$$

In the case of the minimization of the compliance, the mass was naturally introduced as a constraint. However, with the Δl formulation, in an engineering approach, it is more classical to try to reduce the mass while some criteria have to be satisfy

$$\begin{aligned} &\min_{\mathbf{x}} m\left(\mathbf{x}\right) \\ &s.t.\ \Delta l\left(\mathbf{x}, t\right) \leq \Delta l_{max} \\ &\forall t \in [0, T] \end{aligned} \tag{25}$$

Nonetheless, the case where the specifications imposed a maximal mass can also be encountered. In this case, the mass appears as a constraint in the formulation.

The definition of the function Δl is not trivial. For instance, imagine that the tip of a robot have to follow a desired trajectory. The difference between the two trajectories have to be define and this definition influences the convergence behavior of the optimization problem. In Fig. 1, two possibilities are proposed. These definitions need to be investigated to find the most suitable formulation.

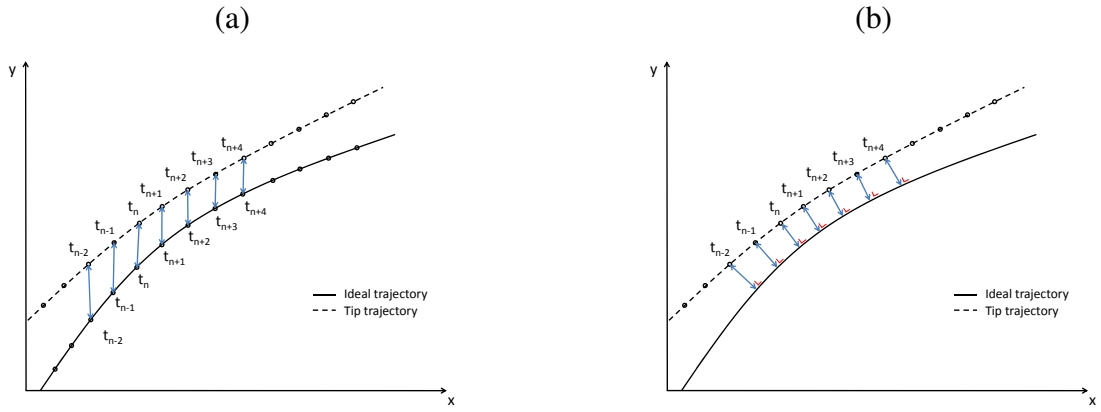

Figure 1: (a) Position difference, (b) Perpendicular difference.

Once the function Δl is defined, it can be introduced without any mathematical treatment in the formulation of the optimization problem. However, mathematical treatments applied to this function can help the convergence. In the next section, the effect of the absolute value function is investigated.

When a constraint on the function Δl is considered at each time step, the number of constraints can be very large. Mathematical treatments can transform these local constraints into a global constraint. A first method is to employ a *Max* function

$$\Delta l\left(\mathbf{x}, t\right) \leq \Delta l_{max} \text{ becomes } \max_{\mathbf{t}} \Delta l\left(\mathbf{x}, t\right) \leq \Delta l_{max} \tag{26}$$

A second possibility is to use an averaged function Δl over the time T

$$\Delta l\left(\mathbf{x}, t\right) \leq \Delta l_{max} \text{ becomes } \frac{1}{T} \int_0^T \left|\Delta l\left(\mathbf{x}, t\right)\right| dt \leq \Delta l_{max} \tag{27}$$

The influence of these mathematical treatments is studied in the next section.

In optimization problems with dynamic loading, taking stress constraints into account strongly increases the number of constraints. Indeed, considering the stresses defined on the elements, the number of stress constraints is equal to the number of elements multiplied by the number of time steps.

$$\boldsymbol{\sigma}\left(\mathbf{x}, \mathbf{P}, t_i\right) \leq \sigma_{max}, \qquad \forall\, i = 1, \ldots, n \text{ and } \forall\, P \in V_E. \tag{28}$$

The shape optimization of a connecting rod under dynamic loading is developed below where the different formulations proposed previously are investigated.

5 NUMERICAL APPLICATIONS

5.1 Modeling of a slider-crank mechanism

The numerical application consists of the optimization of a connecting rod within a slider-crank mechanism, which models a single-cylinder in a four-stroke internal combustion diesel engine (Fig. 2.a). This is the component which links the crank pin of the crankshaft to the piston pin. The connecting rod is the central component which permits the transformation of a translational movement into a rotational movement. The material is steel with a Young modulus of $E = 210$ [GPa], a Poisson ratio of $\nu = 0.3$ and a volumic mass of 7800 [kg/m^3]. The rotation speed of the crankshaft is 4000 [Rpm] for the simulation. At this rotation speed, the dynamic loading due to inertia forces represents about 15% of the loading at the top dead center (explosion).

The numerical simulation is conducted by imposing the rotation speed of the crankshaft which goes from 0 to 4000 [Rpm] in 0.01 [s] in a kinematic simulation (Fig. 2.b). After, the dynamic analysis is performed: a period of 0.0025 [s] is needed to stabilize the dynamic response, then the rotation speed stays at 4000 [Rpm] during one cycle (0.03 [s]) where the gas pressure is introduced. One complete cycle corresponds to a rotation of 720 [°] of the crankshaft. The pressure gas is known from experimental measurements of a real diesel engine at 4000 [Rpm] and is introduced as an external force in the multibody system.

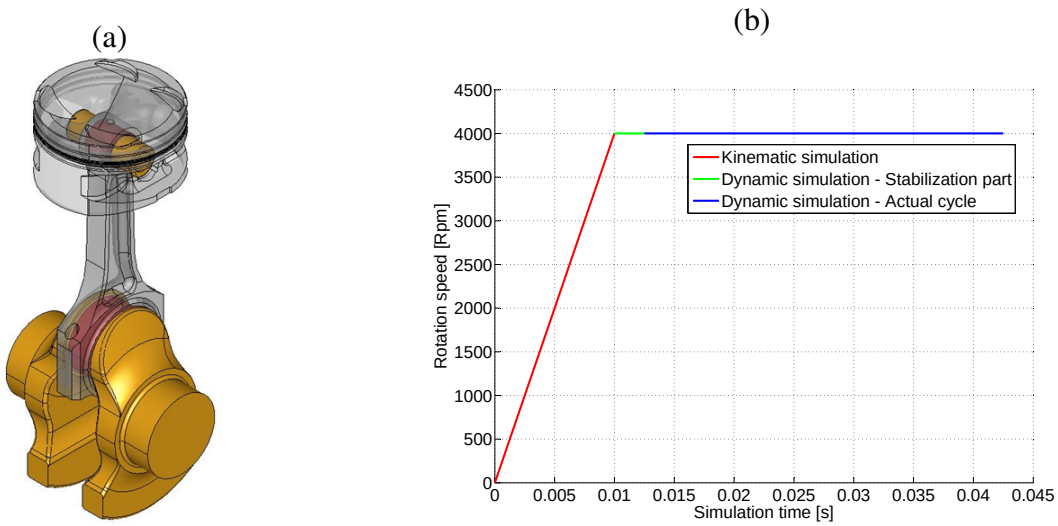

Figure 2: (a) Slider-crank mechanism, (b) Rotation speed of the crankshaft.

The connecting rod is modeled by shell elements with a thickness of 12 [mm] while the crankshaft is considered as rigid. The piston is represented by its mass (0.456 [Kg]) and by a

cylindrical joint. The connecting rod is defined thanks to 7 shape parameters (Fig. 3.a):

$$\mathbf{x} = [D_1\ D_2\ R_1\ R_2\ R_3\ R_4\ R_5]^T \tag{29}$$

A transfinite mesh is used to mesh the connecting rod (Fig. 3.b). The components are linked with ideal kinematic joints. For the time integration, the Chung-Hulbert scheme is used with a time step of 0.001 [s] for the first part of the dynamic analysis while a time step of 0.00025 [s] is adopted for the second part of the dynamic analysis.

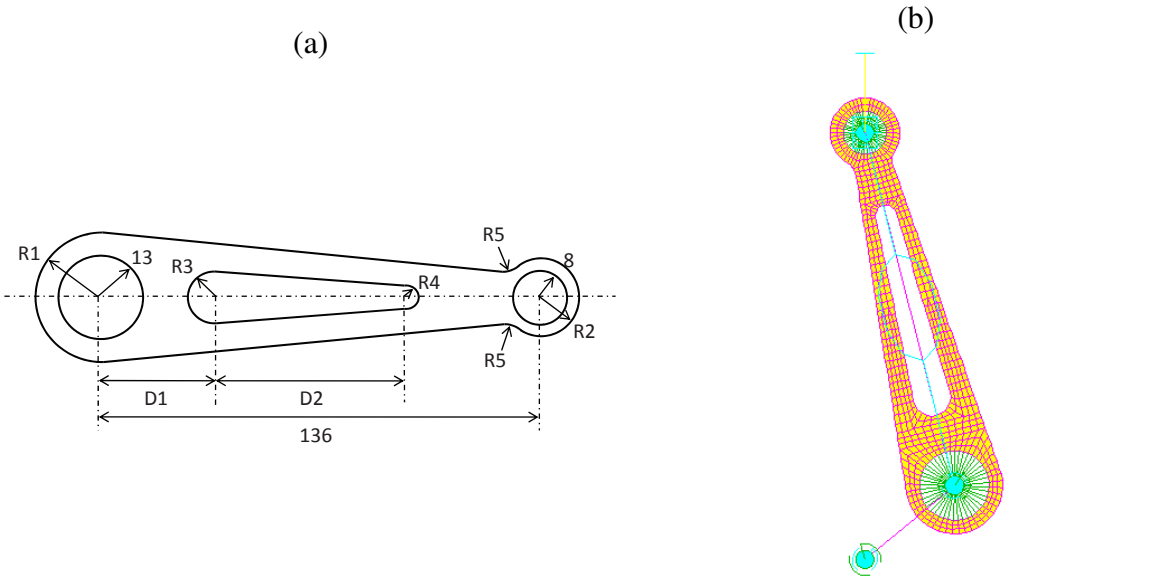

Figure 3: (a) Parametric model of the connecting rod, (b) Finite element model of the slider-crank mechanism.

The connecting rod arises from an engine which has a stroke smaller than the bore. As the engine has a small stroke, the distance between the piston and the valves is reduced at the maximum at the top dead center to obtain the highest compression ratio. Therefore, it is critical to know precisely the elongation of the connecting rod because a too large elongation can destroy the engine.

The displacement of the piston is cyclic and can be formulated by an analytical expression. It is really important to notice that in this case, the framework of the mechanism is known *a priori* if there is no elastic deformation. The formulation of the optimization problem could take profit of this knowledge to formulate the problem in an engineering approach of the design: minimizing the difference between the real trajectory of the connecting rod and the ideal trajectory of a rigid connecting rod. However, the situation is similar to the one in Fig. 1 and a definition should be adopted to express the difference between the two trajectories.

In this case, this problem can be avoided because it is the elongation of the connecting rod which is important. Therefore, the elongation of the connecting rod is taken into account by a distance indicator element between the center of the crank pin to the center of the piston pin. The Δl function is simply the output of the distance indicator element.

Analyzing a typical curve of the elongation of a connecting rod (Fig. 4), the elongation takes place from 480 to 590 [°], i.e. during the exhaust phase. *A priori*, the optimization must place emphasis on this part to minimize the elongation.

In the next section, different formulations for the optimization of the connecting rod are investigated and compared. As the service conditions of the connecting rod are known *a priori*,

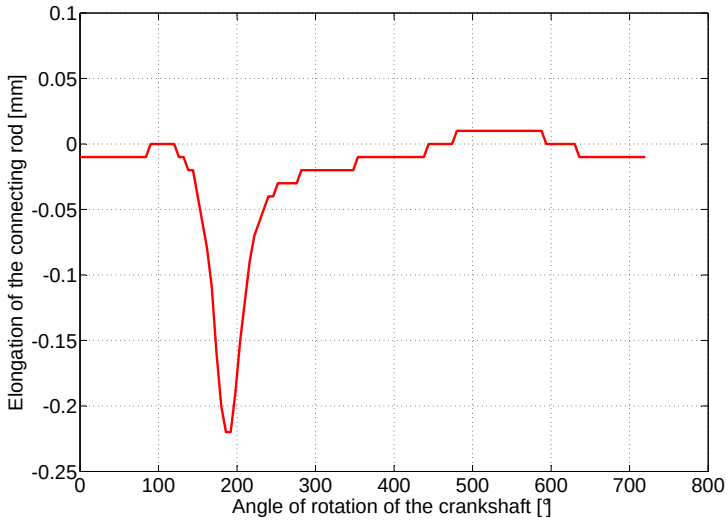

Figure 4: Typical elongation of a connecting rod.

the formulations adopted take profit of this knowledge. Thanks to them, a special attention is payed to stress-optimization.

5.2 Optimization with elongation constraints

5.2.1 Investigation on the elongation formulations

This first numerical application is dedicated to the minimization of the elongation of the connecting rod. With the measure given by the distance indicator element, positive and negative numbers are obtained and one must be aware of this for the formulation of the optimization problem.

The formulations investigated here reflect the engineering approach of the design. The situation is that the specifications impose a maximum elongation and that the goal of the designers is to minimize the mass of the connecting rod while the elongation is kept under this imposed value.

Different formulations are possible to express the elongation during the simulation time. Several possibilities are investigated and compared to determine which one is the most convenient, robust and stable in the case of the optimization of a connecting rod in a reciprocating engine with cyclic dynamic loading.

A first formulation in Eq. (30) is to minimize the mass while the elongation coming from the distance indicator element at each time step is taken into account without any mathematical treatment.

$$\begin{aligned} &\min_{\mathbf{x}} m\left(\mathbf{x}\right) \\ &s.t.\ k\left(\Delta l\left(\mathbf{x}, t_i\right) \leq \Delta l_{max}\right) \\ &\text{with } i = 1, \ldots, \text{nbr time step} \end{aligned} \tag{30}$$

where Δl_{max} is equal to 0.015 [mm]. The k factor is a scaling factor to improve the numerical conditioning of the problem and is equal to 10^6 in this study. Due to the fact that an elongation constraint is considered at each time step, the control level on the design is very high. However,

the high number of constraints makes the optimization problem more complex for the optimizer. As the elongation occurs only during the exhaust phase, it could be interesting to impose elongation constraints only during this period in order to reduce the number of constraints.

Despite the important number of constraints, the optimizer is able to converge in a monotonous and stable way (Fig. 5.a). Nonetheless, the optimization process continues until the maximum number of iterations allowed while the convergence seems to be reached. Observing the constraints on Fig. 5.b, the maximum elongation is lower than the upper bound. This is why the optimization process continues because it can still decrease the mass. Unfortunately, the variables that are very sensitive have reached their optimal value and the variables that can still be modified are not very sensitive. This causes that the convergence of the problem is not totally obtained and continues slowly towards the optimal solution. This problem comes from the criterion that have been chosen to stop the iterative process. Indeed, the default criterion of the optimizer (Boss Quattro) is based on the variations of the design variables. It could be interesting to select the criterion based on the variation of the objective function to stop the iterative process earlier.

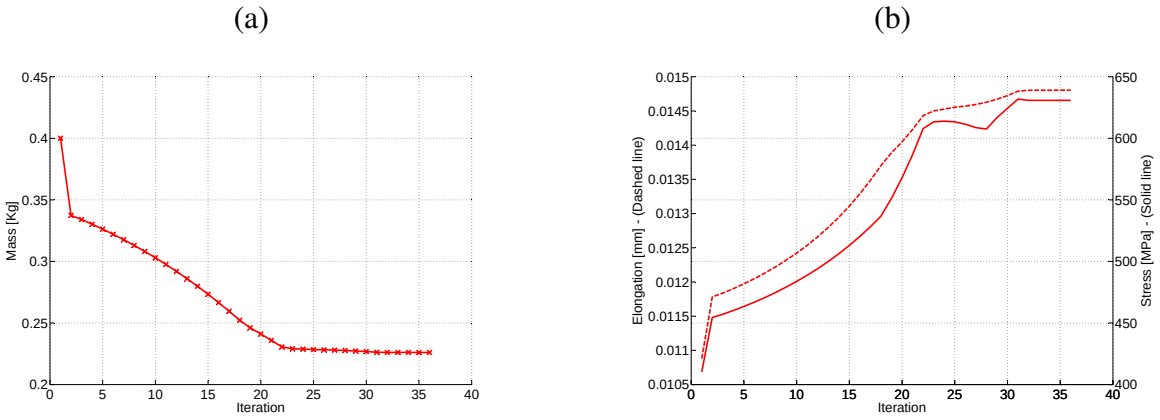

Figure 5: Formulation in Eq. (30): (a) Evolution of the mass, (b) Evolution of the maximum elongation and of the maximal stress.

The second formulation investigated in Eq. (31) is similar to the previous one except that the absolute value of the elongation is considered. This allows having only positive values for the elongation constraints.

$$\begin{aligned} &\min_{\mathbf{x}} m\left(\mathbf{x}\right) \\ &s.t.\ \ k\left(\left|\Delta l\left(\mathbf{x}, t_i\right)\right| \leq \Delta l_{max}\right) \\ &\text{with } i = 1, \ldots, \text{nbr time step} \end{aligned} \tag{31}$$

where Δl_{max} is equal to $0.21\ [\mathrm{mm}]$.

In Fig. 4, it is clearly shown that the connecting rod contracts much more than it elongates. Taking the absolute value of the elongation function, the part where the connecting rod contracts becomes the predominant part. Therefore, the problem is that at the optimal point, the active constraint is not directly related to the maximal elongation but to a maximal contraction. However, this formulation also imposes a limit on the maximal deformation of the connecting rod. The only difference is that the designers need to find a good value of the bound Δl_{max} in order to limit the real elongation of the connecting rod to $0.015\ [\mathrm{mm}]$.

With this formulation, the convergence is very fast, only 12 iterations. Moreover, the convergence curve of the objective function is stable and monotonous. The disadvantage of this formulation is that the value of the upper bound do not correspond to the real value of the maximal elongation which makes the method inadequate.

(a) (b)

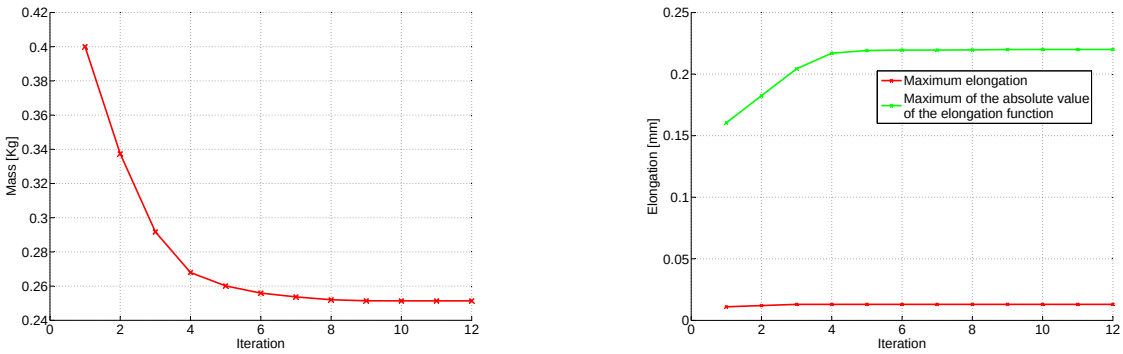

Figure 6: Formulation in Eq. (31): (a) Evolution of the mass, (b) Evolution of the maximum elongation.

The formulations in Eqs. (30-31) are local formulations. An elongation constraint is considered at each time step. The next two formulations are global formulations, i.e. a constraint sums up the elongation constraints at each time step.

The first global formulation in Eq. (32) is expressed with a *Max* function which selects the maximum elongation amongst all the time steps.

$$\begin{gathered} \min_{\mathbf{x}} m\left(\mathbf{x}\right) \\ s.t.\ k\left(\max_{t_i}\left[\Delta l\left(\mathbf{x},t_i\right)\right] \leq \Delta l_{max}\right) \\ \text{with } i=1,\ldots,\text{nbr time step} \end{gathered} \tag{32}$$

This formulation creates a non-smooth function for the constraint and it is important to be aware of this. With the *Max* formulation, it is easy to impose the upper bound on the elongation constraint. In Fig. 7.a, the convergence curve is monotonous and stable. However, the same phenomenon as in the first formulation appears where some design variables, not very sensitive, keep on evolving, which prevents the process to end due to the fact that the end criterion is based on the variations of the variables.

The second global formulation in Eq. (33) is inspired from the work [9]. This formulation takes into account the elongation constraints at each time step but summarizes them in one constraint thanks to a *Mean* function.

$$\begin{gathered} \min_{\mathbf{x}} m\left(\mathbf{x}\right) \\ s.t.\ k\left(\frac{1}{t_{max}}\sum_{i=0}^{t_{max}}\left|\Delta l\left(\mathbf{x},t_i\right)\right| \leq \Delta l_{max}\right) \end{gathered} \tag{33}$$

This formulation has also the advantage that the number of constraints is decreased but the same problem as in the formulation Eq. (31) concerning the value of the upper bound is present.

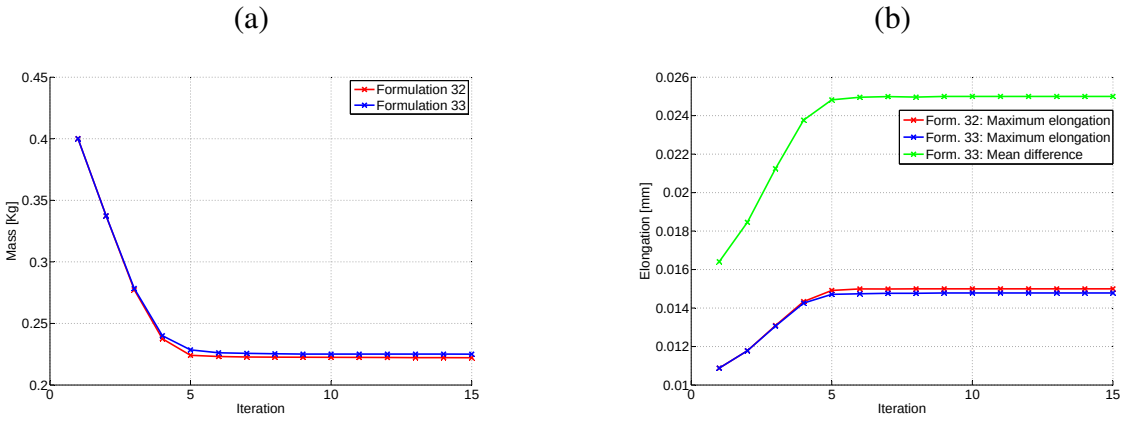

Figure 7: Formulation in Eq. (32-33): (a) Evolution of the mass, (b) Evolution of the elongation.

Indeed, there is no clear relation between the maximum elongation and the mean elongation. Therefore, the upper bound on the mean elongation must be chosen in a way that the maximum elongation is less than 0.015 [mm]. The problem due to the small sensitivities of some variables is also present (Fig. 7.a).

Comparing these global formulations (Fig. 7), their behavior is the same: they are stable and monotonous. The small difference is that the upper bound on the *Mean* formulation do not correspond exactly to the upper bound of 0.015 [mm] on the maximum elongation.

5.2.2 Conclusion on the elongation formulations

Local and global formulations of the elongation have been investigated. For all the formulations, the optimization process converges towards an optimal solution. However, with the formulations in Eqs. (31-33), the value of the upper bound of the constraints is not easy to determine due the lack of a relation between the formulation of the elongation and the maximum elongation. The local formulation in Eq. (30) takes more iterations to converge than the global formulation in Eq. (32) with the *Max* formulation.

In conclusion, despite the fact that the *Max* formulation is non smooth, this formulation is suitable to express this type of optimization problems. To perform these optimization problems, a feasible starting point is selected. The case of an infeasible starting point is discussed in the next section. A last remark is that it is better to use a convergence criterion based on the variation of the objective function rather than on the variations of the design variables.

5.3 Optimization with stress constraints

5.3.1 Investigation on the problem formulation

The second numerical application is dedicated to optimization taking into account stresses. To better capture the stresses and to obtain reliable values of the stress concentrations, the mesh of the previous application is refined. Nevertheless, the influence of the mesh refinement is studied.

A stress constraint imposed at each time step for each element is not reasonable. Indeed, considering a coarse mesh with 600 elements and 120 time steps for the complete cycle, it leads to 72000 restrictions. The trick is that a critical instant is observed for this mechanism. When the explosion occurs, the stresses strongly increase and therefore, the optimization can be bond on stresses at this instant only.

The first formulation in Eq. (34) of this optimization problem is to minimize the mass while the stresses, when the explosion occurs (critical time), are kept under $\sigma_{max} = 550$ [MPa].

$$\begin{aligned} &\min_{\mathbf{x}} m\left(\mathbf{x}\right) \\ &s.t.\ \boldsymbol{\sigma}\left(\mathbf{x}, \mathbf{P}, t_{crit}\right) \leq \sigma_{max} \\ &\text{with } \forall\ P \in V_E \end{aligned} \tag{34}$$

When the mesh is relatively coarse (600 elements), the convergence is fast, monotonous and is realized within the characteristic number of iterations for static structural optimization. When the mesh is refined, from 600 to 3832 elements, the convergence is not monotonous anymore (Fig. 8.a). After a descent part, the mass slightly increases with oscillations then stabilizes. As the stress concentrations are better captured, it is normal that the optimized mass is a little bit heavier.

Concerning the constraints on the stresses (Fig. 8.b), it is observed that the maximal stress, for the coarse mesh, goes until the limit and activates the constraint until the end of the process. For the refined mesh, the maximal stress violates the constraint during the oscillating part of the process and then activates the constraint.

It is interesting to notice that, as the number of constraints increases and makes more complex the optimization problem, the middle part of the optimization process oscillates. The gradient-based method has more difficulties to find the way of convergence. However, even if the optimization process is slower, the process converges.

One must be aware that the simulation with the refined mesh is 3 times slower. The CPU time for the simulation with the coarse mesh is 2 min 55.24 sec while the CPU time is 8 min 28.27 sec with the refined mesh.

(a) (b)

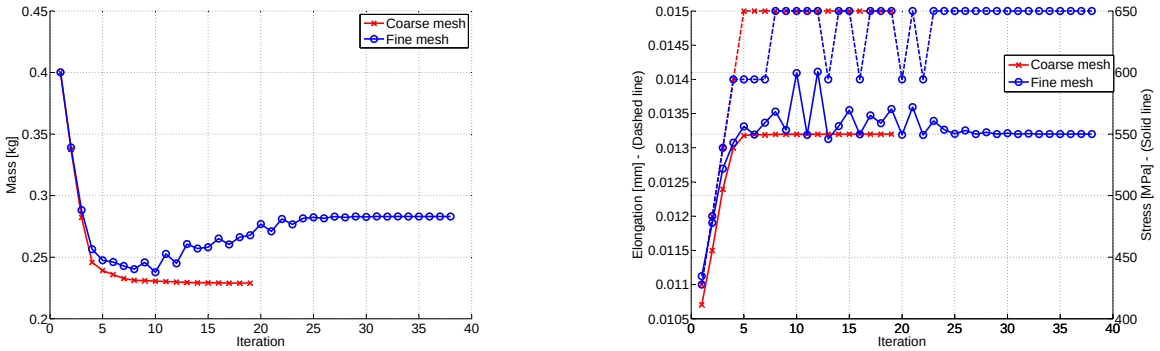

Figure 8: Formulation in Eq. (34): (a) Evolution of the mass, (b) Evolution of the maximum elongation and the maximal stress.

Another type of formulation in Eq. (35) is to minimize the stresses at the critical time while the specifications impose a maximal mass in order to increase, for instance, the fatigue strength.

$$\begin{aligned} &\min \boldsymbol{\sigma}\left(\mathbf{x}, \mathbf{P}, t_{crit}\right) \\ &s.t.\ m\left(\mathbf{x}\right) \leq m_{max} \\ &\text{with } \forall\ P \in V_E \end{aligned} \tag{35}$$

Normally, this problem is similar to the previous one and if the problem is well translated in this formulation, i.e. imposing the right bounds, etc, the optimal solution should be the same. In Fig. 9.a, the convergence is not monotonous for the coarse mesh but it converges in 25 iterations. Concerning the refined mesh, the convergence is monotonous but the process goes until the maximal number of iterations allowed without converging. Indeed, in Fig. 9.b, it is observed that the mass constraint is violated for both optimization processes during the iterations. However, the process with the coarse mesh is able to reduce the mass until activating the constraint while the other process is not able. The mass tends to stabilize despite the fact that its constraint is violated.

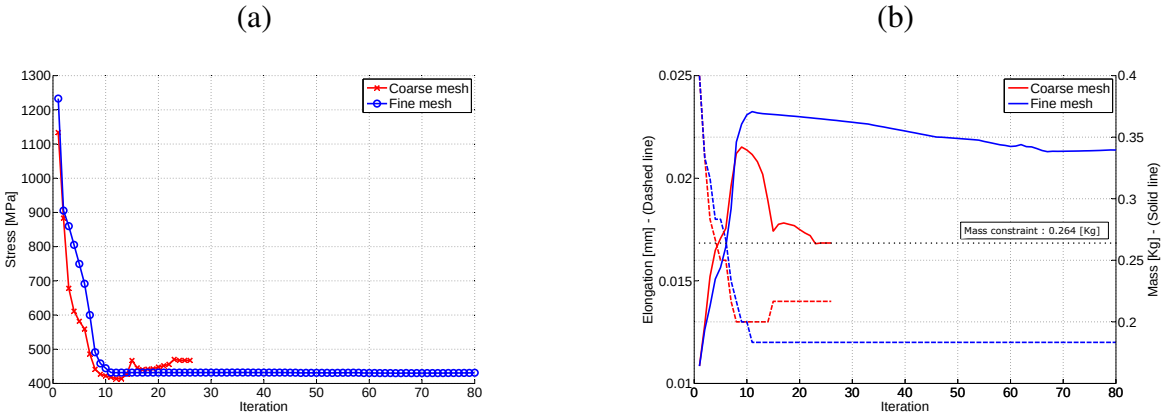

Figure 9: Formulation in Eq. (35): (a) Evolution of the stress, (b) Evolution of the maximum elongation and the mass.

To help the process to converge, a two steps strategy is utilized. First, the optimization is run with the coarse mesh until convergence. Then, the design variables are introduced as the initial starting point for the optimization with the finer mesh. There is no amelioration from the previous case. In 3 iterations, the mass strongly increases and reaches the same mass as the mass of the previous case. The process is not able to converge and the constraint is still violated after the maximum number of iterations allowed.

This technique can be used in the first case (Eq. (34)) to reduce computation time. Indeed, the optimization process was more stable, more robust. Therefore, it is useful to use the coarse mesh in a pre-optimization phase to obtain a good starting point. In a second phase, the refined mesh is employed for the optimization process which allows running the optimization process with a better knowledge of the stress concentrations.

To realize these optimizations, the starting point was always chosen feasible due to the observation that gradient-based methods have more facilities to converge with a feasible starting point [10]. However, it is not always easy to find a feasible starting point. This last case investigates the two previous optimization processes with an infeasible starting point. The coarse mesh is used for this study. It turns out that the first formulation with the minimization of the mass (Eq. (34)) converges even if the starting point is infeasible. The process only needs 4 more iterations (Fig. 10). An interesting point is that, beginning with two different starting points, very far from each other in the design space, leads to the same optimal solution. This may indicate that the optimal solution could be a global optimal solution.

The formulation in Eq. (35) do not converge with an infeasible starting point. The process is not able to increase the level of stresses in the component in order to not violate the mass constraint anymore. With the feasible starting point, the process converged but the convergence

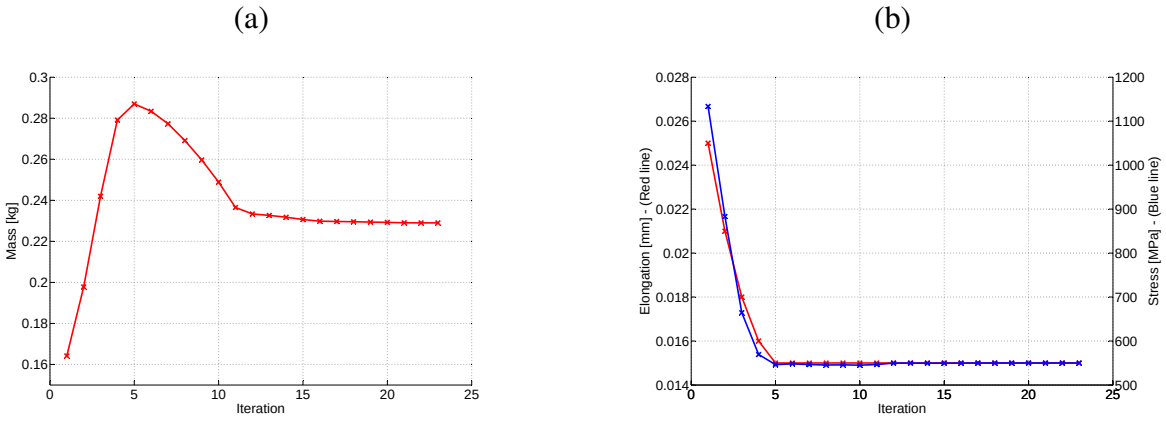

Figure 10: Infeasible starting point (Form. Eq. (34)): (a) Evolution of the mass, (b) Evolution of the maximum elongation and the maximal stress.

was not monotonous. From this observation, one could think that the convergence of optimization process with an infeasible starting can be conclusive when the convergence is at least monotonous and stable with a feasible starting point.

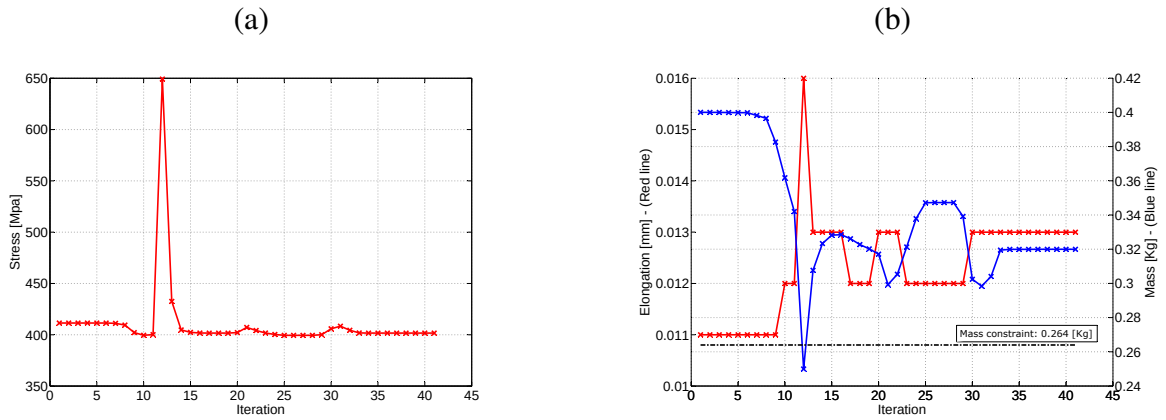

Figure 11: Infeasible starting point (Form. Eq. (35)): (a) Evolution of the Stress, (b) Evolution of the maximum elongation and the mass.

5.3.2 Conclusion on the stress optimization problem

In this second numerical application, two stress-optimization formulations are investigated. Moreover, an analysis of the influence of the mesh refinement has been conducted. It results that the first formulation in Eq. (34) is very robust and is able to take into account a large number of stress constraints. The feasibility of the starting point has also been investigated. It turns out that this formulation is able to converge from an infeasible starting point while the other formulation in Eq. (35) which was less stable with a feasible starting point, do not converge.

6 CONCLUSION AND PERSPECTIVES

This paper is about the optimization of structural components carried out in the framework of flexible multibody systems simulation. The optimization procedure is based on a dynamic analysis of the flexible mechanism. This approach has several advantages. The first is that the

method tries to define as precisely as possible the dynamic loading of the components under service conditions. This follows the actual evolution of virtual prototyping and computational mechanics. The second advantage is that the method is able to take properly the dynamic coupling between large overall rigid-body motions and deformations into account. Only a single dynamic analysis is required by the optimizer while a patchwork of static analysis would be necessary with the equivalent static load approach. Furthermore, design-dependent loading can be considered. This system approach is much richer than a method where the considered component is isolated from the mechanism. Indeed, this approach is able to capture more complex behaviors including component interactions.

The "fully integrated" approach is here extended to the shape optimization of a realistic connecting rod in a reciprocating engine with cyclic dynamic loading. The dynamic loading due to the inertia forces plays a critical role in this study.

The formulations of the objective function and the constraints are investigated in details. The optimization problem formulation is critical for the optimization of dynamic problems and the formulation has to be well-suited to the actual dynamic problem. Robust formulations are proposed for the optimization of the connecting rod regarding its elongation and for its stress-optimization.

In the future, one will have to investigate dynamic stress constraints in flexible multibody systems when a critical time does not exist. A selection of the zones where the stresses are the most important should be considered in order to keep a reasonable number of restrictions. Finally, topology optimization will have to be further investigated under dynamic loading in the light of the results that have been gained in sizing and shape optimization.

7 ACKNOWLEDGMENT

The author Emmanuel TROMME would like to acknowledge Interreg IV Euregio Meuse-Rhin (Automotive Sustainable Training Euregio Project) for its financial support.

REFERENCES

[1] M.P. Bendsoe and O. Sigmund. *Topology optimization: Theory, Methods, and Applications.* Springer Verlag, Berlin, 2003.

[2] D. A. Saravanos and J. S. Lamancusa. Optimum structural design of robotic manipulators with fiber reinforced composite materials. *Computers & Structures*, **36**, 119–132, 1990.

[3] S. Oral and S. Kemal Ider. Optimum design of high-speed flexible robotic arms with dynamic behavior constraints. *Computers & Structures*, **65**(2), 255–259, 1997.

[4] P. Häussler, J. Minx, D. Emmrich. Topology optimization of dynamically loaded parts in mechanical systems: Coupling of MBS, FEM, and structural optimization. Proceedings of NAFEMS Seminar "Analysis of Multi-Body Systems Using FEM and MBS, Wiesbaden, Germany, October 27–28, 2004.

[5] P. Häussler, D. Emmrich, O. Müller, B. Ilzhöfer, L. Nowicki and A. Albers. Automated topology optimization of flexible components in hybrid finite element multibody systems using ADAMS/Flex and MSC.Construct. Proceedings of the 16th European ADAMS Users' Conference, 2001.

[6] B. S. Kang and G. J. Park. Optimization of flexible multibody dynamic systems using the equivalent static load method. *AIAA Journal*, **43**(4), 846–852, 2005.

[7] E.P. Hong, B.J. You, C.H. Kim and G.J. Park. Optimization of flexible components of multibody systems via equivalent static loads. *Structural Multidisciplinary Optimization*, **40**, 549–562, 2010.

[8] M. Géradin and A. Cardona. *Flexible Multibody Dynamics: A Finite Element Approach.* John Wiley & Sons, New York, 2001.

[9] O. Brüls, E. Lemaire, P. Eberhard and P. Duysinx. Topology optimization of structural components included in flexible multibody systems. Proceedings of the 7th World Congress on Structural and Multidisciplinary Optimization, COEX Seoul, Korea, May 21–25, 2007.

[10] P. Duysinx, J. Emonds-Alt, G. Virlez, O. Brüls and M. Bruyneel. Advances in optimization of flexible components in multibody systems: Application to robot-arms design. Proceedings 5th Asian Conference on Multibody Dynamics, Kyoto, Japan, August 23–26, 2010.

[11] O. Brüls, A. Cardona, and M. Géradin. Modelling, simulation and control of flexible multibody systems. *Simulation Techniques in Applied Dynamics*, In W. Schiehlen and M. Arnold, editors, CISM Lecture Notes **507**, 21–74, Springer-Verlag, Wien, 2008.

[12] A. Cardona, M. Géradin and D.B. Doan. Rigid and flexible joint modelling in multibody dynamics using finite elements. *Computer Methods in Applied Mechanics and Engineering*, **89**, 395–418, 1991.

[13] J. Chung and G.M. Hulbert. A time integration algorithm for structural dynamics with improved numerical dissipation: The generalized-α method. *Journal of applied mechanics*, **60**, 371–375, 1993.

[14] M. Arnold and O. Brüls. Convergence of the generalized-α scheme for constrained mechanical systems. *Multibody Systems Dynamics*, **18**(2), 185–202, 2007.

[15] K. Svanberg. A globally convergent version of MMA without line search. Proceedings of the First World Congress of Structural and Multidisciplinary Optimization (WCSMO1), Goslar, Germany, 9–16, 1995.

[16] C. Fleury and V. Braibant. Structural optimization: A new dual method using mixed variables *International Journal for Numerical Methods in Engineering*, **23**, 409–428, 1986.

[17] K. Svanberg. The method of moving asymptotes - a new method for structural optimization *International Journal for Numerical Methods in Engineering*, **24**, 359–373, 1987.

[18] O. Brüls and P. Eberhard. Sensitivity analysis for dynamic mechanical systems with finite rotations. *International Journal for Numerical Methods in Engineering*, **74**(13), 1897–1927, 2008.